Kinetic approach to the cluster liquid-gas transition

F. Calvo
Laboratoire de Physique Quantique, IRSAMC, Université Paul Sabatier, 118 Route de Narbonne, F31062 Toulouse Cedex, France

The liquid-gas transition in free atomic clusters is investigated theoretically based on simple unimolecular rate theories and assuming sequential evaporations. A kinetic Monte Carlo scheme is used to compute the time-dependent properties of clusters undergoing multiple dissociations, and two possible definitions of the boiling point are proposed, relying on the cluster or gas temperature. This numerical approach is supported by molecular dynamics simulations of clusters made of sodium atoms or C_{60} molecules, as well as simplified rate equation.

PACS numbers: 36.40.Qv,82.60.Qr,05.10.Ln

arXiv:physics/0410049 v1 8 Oct 2004

Boiling is often considered as archetypal of first-order phase transitions in bulk matter. Recent experimental evidence [1, 2, 3, 4] suggests that the liquid-gas transition also occurs in finite atomic systems. The caloric curves measured for sodium [1], hydrogen [2] or strontium [3] clusters exhibit a plateau or a backbending, believed to be signatures of a phase transition rounded by size effects. Similar conclusions have been inferred from collisions between gold nuclei [5]. The experiments performed by Pochodzalla and coworkers have since motivated a significant amount of theoretical work to help the search for a possible equation of state for nuclear matter [6, 7, 8, 9, 10].

For more than two decades, fragmentation has been recognized as one of the most convenient ways of accessing fundamental cluster properties such as binding energies or temperatures. These quantities were related to each other through calorimetric experiments on the solid-liquid phase change [11, 12]. The crucial role of the observation time was also noticed at an early stage, and more fully understood by Klots [13] who introduced the concept of the evaporative ensemble. Free clusters are never strictly stable when their energy exceeds a certain dissociation threshold, as fragmentation will occur, possibly very late. Measurements on free clusters are thus conducted on species resulting from hotter and bigger clusters, and which have sufficiently cooled down so as not to evaporate further. Unfortunately, the relatively long times involved in experiments (usually the μs–ms range) have prevented Klots' ideas from being exploited in later theoretical studies. While melting can be conveniently addressed using Monte Carlo (MC) or molecular dynamics (MD) simulations by artificially keeping the cluster in a container [14], fragmentation of a cluster into vacuum is an out-of-equilibrium phenomenon. The difficulty of accounting for the time variable has generally been circumvented by considering lattice-gas or percolation models [8, 10] as well as periodic boundary conditions [6, 9].

Unimolecular rate theories provide a general framework to describe single dissociation events accurately and over long time scales [15]. Here we introduce a kinetic Monte Carlo (KMC) scheme based on such rate theories to calculate the caloric curves of clusters across the liquid-gas transition for arbitrarily long observation times.

We start by illustrating the boiling problem by showing the results of classical MD simulations carried out on three selected clusters, namely Na_{55}, $(C_{60})_{40}$, and a model binary cluster $X_{13}Y_{42}$. These systems are described using an explicit many-body potential [16], the Girifalco potential [17], and Lennard-Jones (LJ) interactions, respectively. For the LJ cluster, we chose $\varepsilon_{XX} = 1$, $\varepsilon_{YY} = 1/2$ and $\varepsilon_{XY} = 1/\sqrt{2}$, all distance units and masses being set to one. For each cluster, MD trajectories are performed starting from the lowest-energy minimum, at increasing total energies and zero angular and linear momenta. After some observation time t we determine the biggest remaining cluster as the largest set of connected atoms or molecules, two atoms being connected when their distance is smaller than a cut-off value $r_{\rm cut}$ chosen as twice the equilibrium distance. The instantaneous temperature of this cluster is then calculated after removing the overall translation and rotation contributions. The average cluster size and temperature obtained over 100 independent trajectories (20 for the longest waiting times) are represented for the three clusters in Fig. 1.

All caloric curves exhibit two clearly distinct regimes. At low energies, the roughly linear increase of temperature characterizes the condensed phases as solidlike and liquidlike. For the sodium and, to a lesser extent, for the LJ cluster, a small inflection marks the onset of melting. At high energies, the cluster temperature drops and reaches a plateau. The plateau temperature is lower and the change between the two regimes is sharper as the waiting time increases. This behavior is consistent with the observed smaller average cluster size, and results from a stronger evaporative cooling. In the cluster of fullerene molecules, no evidence for the melting transition is seen on the caloric curves, in agreement with the lack of stability of the liquid phase known in bulk C_{60} [18]. The backbending seen for the shortest waiting time (0.5 ns) was confirmed by another set of 100 independent MD trajectories. However, without any container preventing dissociation, it is hard to attribute this feature to melting

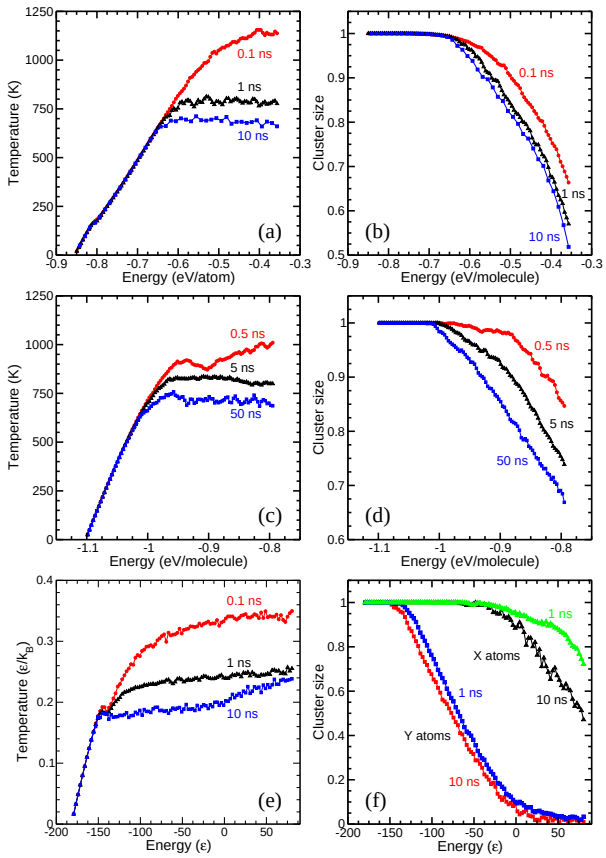

FIG. 1: Caloric curves and average cluster size after various waiting times in MD simulations. (a) and (b) Na_{55}; (c) and (d) $(C_{60})_{40}$; (e) and (f) binary LJ cluster $X_{13}Y_{42}$. Cluster sizes are given relative to the initial size.

or to boiling. The binary LJ cluster was constructed as a two-layer icosahedron, with the most strongly bound atoms X in the center. Provided that the waiting time is long enough, X atoms may dissociate, but only after the Y atoms have evaporated. The fragmentation of X atoms is shown on the caloric curve corresponding to $t = 10$ ns by the slight increase at high excitation energies.

The time-dependence of fragmentation caloric curves can also be calculated from simple cluster models, similar to those introduced by Bixon and Jortner for the isomerization problem [19]. Our first assumption is that clusters are heated adiabatically, allowing fragmentation to occur through sequential loss of monomers [20]. We use simple rate theories to describe each dissociation step. The dissociation rate $k_n(E_n)$ of cluster X_n into X_{n-1} depends on the dissociation energy Δ_n and the total energy E_n through the harmonic RRK approach [21], namely $k_n(E_n) = \nu_0(1 - \Delta_n/E_n)^{3n-6}$. This well known formula contains a single time scale parameter ν_0, related to the typical vibrational period. Once evaporation has occured, the cluster loses a part of its internal energy, which is described more accurately using the Weisskopf theory [22]. The probability distribution of the kinetic energy released (KER), $p_n(\varepsilon, E_n)$, is $p_n(\varepsilon, E_n) \propto \varepsilon(E_n - \Delta_n - \varepsilon)^{3n-7}$. The dissociation of rigid molecules would be described similarly, changing the factor ε and the number $3n-7$ of degrees of freedom to $\varepsilon^{3/2}$ and $5n-7$ for linear molecules, and to ε^2 and $6n-7$ for tridimensional molecules, respectively.

The problem can be further simplified by assuming that the lifetime of the parent cluster is $1/k_n$ and that evaporative cooling removes the average KER $\langle\varepsilon\rangle_n = 2(E-\Delta_n)/(3n-7)$, leading to the energy of the product X_{n-1}, $E_{n-1} = E_n - \Delta_n - \langle\varepsilon\rangle_n$. The multifragmentation problem is thus reduced to computing all successive dissociation rates, from which the survival probabilities $p_n(t)$ of all cluster sizes are calculated following a master rate equation $dp_n/dt = k_n p_n - k_{n-1}p_{n-1}$, solved exactly. A similar "mean-field" technique was used by Hervieux *et al.* to calculate branching ratios in the collision-induced fragmentation of Na_9^+ [23].

Beyond this approximate treatment, the kinetic Monte Carlo method [24] accounts for the continuous character of dissociation times and KER distributions. Starting with the parent cluster size n at total energy E_n, the evaporation rate $k_n(E_n)$ is calculated and the KER ε is chosen randomly from the distribution $p_n(\varepsilon, E_n)$. The energy is decreased by $\Delta_n + \varepsilon$, and the time is updated by the quantity $-\log(\texttt{ran})/k_n$, where $0 \le \texttt{ran} < 1$ is a random real number. This process is iterated until either the waiting time has been exceeded or the remaining energy is below the next dissociation limit. The final cluster has k atoms and the energy E_k, its temperature is obtained in the harmonic approximation $k_B T_k = E_k/(3k-6)$.

The KMC and mean-field methods have been compared on the simplest case of the multiple dissociation of a 100-particle model cluster with $\Delta_n = 1$ for all n. Figs. 2(a) and (b) show the caloric curve and the average final cluster size obtained from the KMC calculations. The mean field values were not reported, as they are undistinguishable from the stochastic data. It should be noted that these results are not significantly affected when the energetics of dissociation are described using RRK theory, $p_n(\varepsilon, E_n) \propto (E_n - \Delta_n - \varepsilon)^{3n-6}$.

The MD results of Fig. 1 are well reproduced by the predictions of this simple model, especially the plateau of the vapor phase and the increasing sharpness of the transition for long observation times. The absence of any feature on the caloric curve for $t \to 0$ demonstrates the kinetic character of the cluster liquid-gas transition. On the other hand the asymptotic curve for $t \to \infty$ exhibits multiple tiny backbendings corresponding to consecutive dissociations leaving the cluster perfectly cold. We have simulated the effect of a more stable cluster at size $n^* = 90$ by imposing $\Delta_{n^*} = 1.5$. The influence of this magic cluster on the curves of Figs. 2(c) and (d) is rather local. The greater stability of the X_{n^*} cluster induces a delay on the subsequent dissociations, but the overall plateau

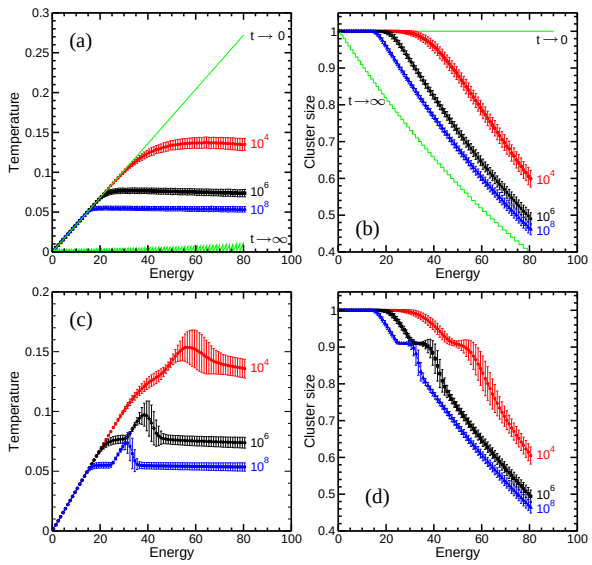

FIG. 2: Caloric curves and average final cluster size obtained from KMC calculations for model clusters without (a and b) or with (c and d) a specially stable fragment at $n = 90$. The waiting times are given in units of $1/\nu_0$, and the cluster sizes are relative to the initial size 100.

temperatures do not vary much.

The kinetic Monte Carlo method can be used in more general situations, for which the rate equation approach is not practical. Clusters with competing fragmentation channels turn into products having different internal energies depending on their history. For instance, heterogeneous clusters X_nY_p can dissociate in multiple ways:

$$\begin{array}{ccccccc} & & & X_nY_p & & & \\ & & \swarrow & & \searrow & & \\ & X_{n-1}Y_p & & & & X_nY_{p-1} & \\ \swarrow & & \searrow & & \swarrow & & \searrow \\ \cdots & & & X_{n-1}Y_{p-1} & & & \cdots \end{array}$$

Statistically the $X_{n-1}Y_{p-1}$ fragment does not have the same energy depending on whether it was produced from $X_{n-1}Y_p$ or from X_nY_{p-1}. For the above example, and within the Weisskopf theory, do the two average energies of the $X_{n-1}Y_{p-1}$ product differ by

$$\Delta E_{n-1,p-1} = 2(\Delta_X - \Delta_Y) \times \frac{3(n+p)-12}{[3(n+p)-7]\cdot[3(n+p)-10]}, \quad (1)$$

depending on which of X or Y was emitted first. Only at large sizes or for similar binding energies $\Delta_X \simeq \Delta_Y$ the two fragmentation routes become equivalent. Moreover, clusters may be prepared at fixed temperature rather than fixed energy. The initial energy is then randomly picked from the canonical distribution $\rho_n(E) \propto E^{3n-6}\exp(-E/k_BT)$ as the first Monte Carlo step.

By mimicking the actual dissociation cascade followed by each individual cluster, the KMC technique offers a realistic statistical description of multifragmentation. The caloric curves of model binary clusters X_nY_{100-n} were calculated assuming that X and Y atoms are bound to the clusters by the energies $\Delta_X = 1$ and $\Delta_Y = 1/2$, respectively. The caloric curves represented in Fig. 3(a) for several compositions exhibit two steps, each associated with the boiling of Y, then X particles. This two-step liquid-gas transition is somewhat similar to the multistep melting process often seen in cluster simulations [25]. As more Y atoms are added, a larger energy is required to evaporate them, therefore the gas transition of the remaining X cluster is initiated at higher temperatures. The different onsets of boiling for X and Y particles in Fig. 1(c) and (d) confirm this two-step transition.

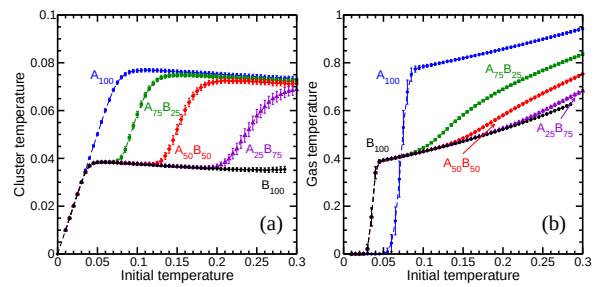

FIG. 3: Final cluster (a) and gas (b) temperatures versus initial temperature in the boiling transition of model binary clusters with various compositions, for the waiting time $10^6/\nu_0$.

We now address possible definitions of the boiling temperature, based on the previous results. The onset of the drop in the slope of the caloric curve provides one possible estimate. However, especially at short waiting times, the variations of the average remaining cluster size seem to be more reliable. Another observable consists of looking at the kinetic energy of the evaporated atoms, in a fashion somewhat more closely related to experimental conditions. Using the same notation as above for the initial and final cluster sizes and energies, and assuming that all $n-k$ evaporated atoms behave like a perfect gas, a gas temperature can be defined by $3(n-k)k_BT/2 = E_n - E_k$.

The variations of the average gas temperature across the boiling transition are shown in Fig. 3(d) for the model binary clusters. Boiling is made evident by the sudden increase of the gas temperature, which provides us with another characterization of the liquid-gas point. The second boiling point involving the more strongly bound X atoms does not lead to significant variations of the gas temperature, because X and Y atoms contribute equally once in the gas phase. A better estimate of the liquid-gas transition temperature of the cluster of X atoms is found with the variations of its final size [see Fig. 1(d)].

The three aforementioned definitions of the boiling point yield similar values in a broad range of situations

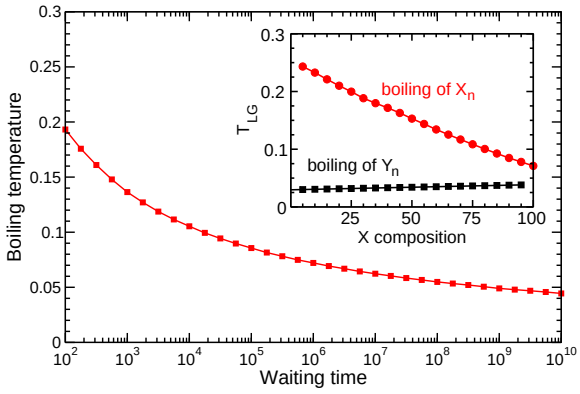

FIG. 4: Boiling temperature of model 100-atom homogeneous cluster versus waiting time. Inset: boiling temperatures of the X and Y parts of model X_nY_{100-n} clusters versus composition n, for the waiting time $t = 10^6/\nu_0$.

covered by our simple models. The dependence of the observation time on the boiling temperature of the homogeneous cluster is represented in Fig. 4. As expected, waiting longer favors evaporation, hence a lower boiling temperature. In most experiments [1, 2, 3, 4] the waiting time is at least 5 orders of magnitude larger than the typical vibrational period. Fig. 4 suggests that the results of these experiments should remain stable by less than 5% if the waiting time is doubled or halved. However, similar measurements on trapped clusters might show some deviation since the trapping time may exceed seconds [26].

In Fig. 4 we also show how the presence of more weakly bound (Y) atoms influence the boiling point of an (X) cluster. The fragmentation temperature of Y atoms does not significantly change with their initial composition. However, as more Y atoms are added, the X product gets progressively colder due to the more numerous evaporations. This explains why the boiling temperature of the X cluster decreases with its composition.

The KMC technique outlined in this paper could be improved using more accurate unimolecular rate theories, such as Phase Space Theory, which incorporates anharmonic densities of states as well as a rigorous treatment of angular momentum constraints [15]. The main assumption of the present approach is that boiling in slowly heated clusters occurs sequentially. Our simulation results seem to validate this hypothesis. As in glasses [27], the arbitrarily long time scales reached by the present statistical approach make it a useful alternative to molecular dynamics. We believe that it forms a bridge between unimolecular rate descriptions and multifragmentation models that assume thermal equilibrium.

As a first application of the KMC method to the cluster dissociation problem, we have considered the liquid-gas transition. Our results emphasize the important role played by the observation time on the caloric curves. They also indicate that multiple-step boiling transitions could be detected in heterogeneous clusters. Beyond these examples, a more complete interpretation of recent experiments [1, 2, 3], especially on clusters exhibiting competing dissociation channels [4], could be anticipated.

[1] M. Schmidt, T. Hippler, J. Donges, W. Kronmüller, B. von Issendorff, H. Haberland, and P. Labastie, Phys. Rev. Lett. **87**, 203402 (2001).
[2] F. Gobet, B. Farizon, M. Farizon, M. J. Gaillard, J. P. Buchet, M. Carré, P. Scheier, and T. D. Märk, Phys. Rev. Lett. **89**, 183403 (2002).
[3] C. Bréchignac, Ph. Cahuzac, B. Concina, and J. Leygnier, Phys. Rev. Lett. **89**, 203401 (2002).
[4] G. Martinet, S. Díaz-Tendero, M. Chabot, K. Wohrer, S. Della Negra, F. Mezdari, H. Hamrita, P. Désesquelles, A. Le Padellec, D. Gardés, L. Lavergne, G. Lalu, X. Grave, J. F. Clavelin, P.-A. Hervieux, M. Alcamí, and F. Martín, Phys. Rev. Lett. **93**, 063401 (2004).
[5] J. Pochodzalla *et al.*, Phys. Rev. Lett. **75**, 1040 (1995).
[6] D. H. E. Gross, Rep. Prog. Phys. **53**, 605 (1990).
[7] M. Belkacem, V. Latora, and A. Bonasera, Phys. Rev. C **52**, 271 (1995).
[8] X. Campi and H. Krivine, Nucl. Phys. A **620**, 46 (1997).
[9] A. Strachan and C. O. Dorso, Phys. Rev. C **59**, 285 (1999).
[10] Ph. Chomaz, V. Duflot, and F. Gulminelli, Phys. Rev. Lett. **85**, 3587 (2000).
[11] M. Schmidt, R. Kusche, W. Kronmüller, B. von Issendorff, and H. Haberland, Phys. Rev. Lett. **79**, 99 (1997).
[12] A. A. Shvartsburg and M. F. Jarrold, Phys. Rev. Lett. **85**, 2530 (2000); G. A. Breaux, R. C. Benirschke, T. Sugai, B. S. Kinnear, and M. F. Jarrold, Phys. Rev. Lett. **91**, 215508 (2003).
[13] C. E. Klots, J. Chem. Phys. **83**, 5854 (1985).
[14] J. K. Lee, J. A. Barker, and F. F. Abraham, J. Chem. Phys. **58**, 3166 (1973).
[15] S. Weerasinghe, F. G. Amar, J. Chem. Phys. **98**, 4967 (1993).
[16] Y. Li, E. Blaisten-Barojas, and D. A. Papaconstantopoulos, Phys. Rev. B **57**, 15519 (1998).
[17] L. A. Girifalco, J. Phys. Chem. **96**, 858 (1992).
[18] C. Caccamo, D. Costa, and A. Fucile, J. Chem. Phys. **106** 255 (1997).
[19] M. Bixon and J. Jortner, J. Chem. Phys. **91**, 1631 (1989).
[20] This hypothesis has recently been verified numerically on Lennard-Jones clusters, see J. Chem. Phys. **121**, 819 (2004).
[21] O. K. Rice and H. C. Ramsperger, J. Am. Chem. Soc. **50**, 617 (1928); L. S. Kassel, J. Phys. Chem. **32**, 225 (1928).
[22] V. Weisskopf, Phys. Rev. **52**, 295 (1937).
[23] P. A. Hervieux, B. Zarour, J. Hanssen, M. F. Politis, and F. Martín, J. Phys. B: At. Mol. Opt. Phys. **34**, 3331 (2001).
[24] A. B. Bortz, M. H. Kalos, and J. L. Lebowitz, J. Comput. Phys. **17**, 10 (1975).
[25] F. Calvo and F. Spiegelman, Phys. Rev. Lett. **82**, 2270 (1999); **89**, 266401 (2002).
[26] S. Krückeberg, D. Schooss, M. Maier-Borst, and J. H.

Parks, Phys. Rev. Lett. **85**, 4494 (2000).
[27] J. Hernández-Rojas and D. J. Wales, J. Non-Cryst. Solids **336**, 218 (2004).